

The critical scalarization and descalarization of black holes in a generalized scalar-tensor theory

Yunqi Liu,^{1,*} Cheng-Yong Zhang,^{2,†} Qian Chen,^{3,‡} Zhoujian Cao,^{4,5,§} Yu Tian,^{3,6,¶} and Bin Wang^{1,7,***}

¹*Center for Gravitation and Cosmology, College of Physical Science and Technology, Yangzhou University, Yangzhou 225009, China*

²*Department of Physics and Siyuan Laboratory, Jinan University, Guangzhou 510632, China*

³*School of Physical Sciences, University of Chinese Academy of Sciences, Beijing 100049, China*

⁴*Department of Astronomy, Beijing Normal University, Beijing 100875, China*

⁵*School of Fundamental Physics and Mathematical Sciences,*

Hangzhou Institute for Advanced Study, UCAS, Hangzhou 310024, China

⁶*Institute of Theoretical Physics, Chinese Academy of Sciences, Beijing 100190, China*

⁷*Shanghai Frontier Science Center for Gravitational Wave Detection,*

Shanghai Jiao Tong University, Shanghai 200240, China

We study the critical dynamics in the scalarization and descalarization in the fully nonlinear dynamical evolution in a general theory with scalar field coupling with both Gauss-Bonnet invariant and Ricci scalar. We explore how the Gauss-Bonnet term triggers the black hole scalarization. A typical type I critical phenomenon is observed, where an unstable critical solution emerges at the threshold and acts as an attractor in the dynamical scalarization. In the descalarization, a marginally stable attractor exists at the threshold of the first order phase transition in shedding off black hole hair. This is a new type I critical phenomenon in the black hole phase transition. Implications of these findings are discussed from the perspective of thermodynamic properties and perturbations for static solutions. We examine the effect of scalar-Ricci coupling on the hyperbolicity in the fully nonlinear evolution and find that such coupling can suppress the elliptic region and enlarge parameter space in computations.

Introduction. One of the fascinating topics in general relativity is the black hole (BH) no-hair theorem. Recently an attempt to challenge this theorem has been achieved by considering a quadratic scalar field coupling with the Gauss-Bonnet (GB) [1–7] or Maxwell invariant [8]. At linear level such coupling can trigger tachyonic instability, which spontaneously scalarizes a bald BH (BBH) through a second order phase transition. Besides scalarization, dynamical descalarization through second order phase transition was observed in black hole binaries [9, 10]. Considering higher order scalar coupling, it was found that in the fully nonlinear evolution both scalarization and descalarization can happen more violently through a first order phase transition in both scalar-GB (sGB) [11–13] and Einstein-Maxwell-scalar (EMS) theories [14–18]. In EMS theory critical dynamics in different orders of phase transitions to realize scalarization and descalarization were explored thoroughly in [17, 18]. At the threshold of perturbation, the critical solution (CS) in the first order phase transition was uncovered resembling the type I critical gravitational collapse [19–22]. The discovery of critical phenomena in the scalarization and descalarization enriched the study of critical dynamics in gravity.

It is intriguing to investigate the critical dynamics in a theory with coupling between scalar field and GB term, and reveal the intrinsic mechanism on its scalarization and descalarization. A theory with scalar-GB coupling is of interest to astrophysics [23–28], however most astrophysical tests of scalarized BHs (SBHs) induced by GB term limited in stationary solutions and linear perturbations [29–31].

Numerically the study of nonlinear dynamics in a theory with the scalar-GB coupling is more difficult than that in the EMS theory, due to the lack of well-posedness of the Cauchy problem [32–36]. To avoid the ill-posed dynamical evolution, one limited the study in the weak coupling regime

[9–13, 37, 38] or adopted small parameter space to escape the problematic regions [39–42]. A weak completion dubbed as fixing-the-equations was proposed to reduce the mathematical pathologies and allow one to push the evolution further [43]. A perturbative analysis showed that including the scalar-Ricci coupling can reduce the region of parameter space where hyperbolicity breaks down [44]. This coupling was proposed in neutron star scalarization study [45–47] and it was shown crucial for observational viability [48–50]. It is worth examining the effect of such scalar-Ricci coupling on the hyperbolicity in the fully nonlinear evolution and studying its role to uncover the critical dynamics in scalarization and descalarization in a theory with scalar-GB coupling.

In this letter, we study dynamical critical behaviors in scalarization and descalarization in a generalized theory with a scalar field coupling with both the Ricci scalar and the GB invariant. We show how the GB term triggers the nonlinear scalarization, makes a linearly stable BBH evolve to an unstable SBH attractor and finally transform to a linearly stable SBH. We demonstrate that the property of the CS in the scalarization qualitatively resembles that in the EMS theory. Remarkably, we reveal novel critical behavior in the dynamical descalarization. The CS at the threshold of descalarization is marginally stable and plays the role of a marginal stable attractor, reflecting a new type I critical phenomenon in the black hole phase transition. We disclose the thermodynamic properties and perturbations for static solutions to help understand such novel phenomenon more deeply in the phase transitions. Further, the effect of the scalar-Ricci coupling on the hyperbolicity in the fully nonlinear evolution is investigated.

Setup. We consider a generalized scalar-tensor theory with

action [44, 48–51]

$$S = \frac{1}{16\pi} \int d^4x \sqrt{-g} \left[R - \frac{1}{2}(\partial\phi)^2 + f(\phi)(\beta R + \mathcal{G}) \right], \quad (1)$$

where a scalar field ϕ non-minimally couples to both the Ricci scalar R and the GB invariant $\mathcal{G} = R^2 - 4R_{\mu\nu}R^{\mu\nu} + R_{\mu\nu\alpha\beta}R^{\mu\nu\alpha\beta}$ by $f(\phi)$, β is a dimensionless parameter. The BBH is a solution if $f(0) = 0$, $\frac{df}{d\phi}(0) = 0$. The positive and sufficient large $\frac{d^2f}{d\phi^2}(0)\mathcal{G}$ can trigger a tachyonic instability and spontaneously scalarize the BBH. It was found that at the linear level the coupling between a scalar field and the Ricci scalar can have significant influence on the black hole scalarization [44, 50, 51]. Here we discuss for the first time the fully nonlinear evolution, examine the crucial influence of the scalar-Ricci coupling on the scalarization and its effect on the hyperbolicity of equations of motion. We focus on the coupling function

$$f(\phi) = \frac{\lambda^2}{4\kappa}(1 - e^{-\kappa\phi^4}), \quad (2)$$

where λ, κ are coupling strength parameters. It satisfies $\frac{d^2f}{d\phi^2}(0) = 0$ so that the BBH does not suffer linear tachyonic instability. However, we will show that the BBH becomes unstable against large scalar perturbation and evolves into the SBH.

The equation of motion for gravity can be written as $R_{\mu\nu} - \frac{1}{2}Rg_{\mu\nu} = T_{\mu\nu}^{eff}$ in which the effective energy momentum tensor

$$\begin{aligned} T_{\mu\nu}^{eff} = & \frac{1}{2}\partial_\mu\phi\partial_\nu\phi - \frac{1}{4}g_{\mu\nu}(\partial\phi)^2 \\ & + 2\delta_{\rho\sigma\tau\eta}^{\alpha\beta\gamma\delta}R_{\gamma\delta}^{\tau\eta}\delta_{(\mu}^\sigma g_{\nu)\beta}\nabla^\rho\nabla_\alpha f \\ & - \beta[fG_{\mu\nu} + (g_{\mu\nu}\nabla_\alpha\nabla^\alpha - \nabla_\mu\nabla_\nu)f]. \end{aligned} \quad (3)$$

Here $\delta_{\rho\sigma\tau\eta}^{\alpha\beta\gamma\delta}$ is the generalized Kronecker delta tensor and $G_{\mu\nu}$ the Einstein tensor. The scalar field equation reads

$$\nabla_\mu\nabla^\mu\phi + \frac{1}{2}(\beta R + \mathcal{G})\frac{\partial f}{\partial\phi} = 0. \quad (4)$$

Numerical results of dynamical evolutions. To study the nonlinear dynamics of BH in spherically symmetric spacetime, we use the Painlevé-Gullstrand coordinate ansatz

$$ds^2 = -\alpha^2dt^2 + (dr + \zeta\alpha dt)^2 + r^2(d\theta^2 + \sin^2\theta d\varphi^2). \quad (5)$$

where α, ζ are functions of (t, r) , the apparent horizon r_h is determined by $\zeta = 1$. For a Schwarzschild BH $\alpha = 1, \zeta = \sqrt{\frac{2M}{r}}$ and $r_h = 2M$, where M is BH mass. We consider the nonlinear evolution of a Schwarzschild BH started with mass $M_0 = 1$ perturbed by an initial scalar pulse

$$\phi_0 = 10^{-3}p(r-r_1)^2(r-r_2)^2e^{-\frac{1}{r-r_1}-\frac{1}{r_2-r}}, P_0 = \partial_r\phi_0, \quad (6)$$

when $r \in (r_1, r_2)$, and zero otherwise. We set $r_1 = 8, r_2 = 18$ in this work. The parameter p takes control of

the perturbation amplitude. After the injection of the initial pulse, the total mass of the system is represented by M , the difference $\delta M = M - M_0$ increases monotonically with p . Some other forms of initial pulses have been considered, we achieved qualitatively the same results as what will be presented in the following. Details on the numerical method please see supplemental material.

Without loss of generality, hereafter we present the results with $\lambda = \frac{50}{3}$, $\beta = -\frac{5}{2}$ and $\kappa = 1000$. After the injection of initial pulse, the resultant spacetime keeps a Schwarzschild BH if $p < p_s \approx 0.1355610542323$. When the scalar injection is strong enough, whose amplitude increases within the range $p_s < p < p_d \approx 0.2438$, Schwarzschild BHs become unstable and evolve into SBHs eventually. p_s and p_d are thresholds for the scalarization and descalarization, respectively. Both of them are computed by the bisection method. For the numerical limitation, it is time consuming to improve p_d to higher precision. When $p > p_d$, the infall of strong perturbation makes the BH more massive, so that the GB term $\mathcal{G} \propto M^{-4}$ becomes too small near the horizon. The induced effective potential barrier cannot confine the scalar hair near the horizon. As a result, eventually most of the scalar injection is absorbed by the BH and the spacetime finally evolves into a BBH, but becomes more massive.

Dynamical critical behaviors for scalarization. In order to examine the critical dynamics in the scalarization, we fine tune the perturbation amplitude around p_s and investigate the nonlinear scalarization process. The scalar field evolution is illustrated in Fig.1. Initially the scalar field moves towards a BBH and induces a violent turbulence near the BBH. Then the system evolves to an intermediate state approximated by the critical solution at the threshold p_s ,

$$\phi_p(t, r) \approx \phi_s(r) + (p - p_s)e^{\omega_s t}\delta\phi_s(r) + \text{stable modes}, \quad (7)$$

where $\phi_s(r)$ denotes the scalar distribution of the CS, $\delta\phi_s(r)$ is the single unstable eigenmode with positive eigenvalue $\omega_s \simeq 0.106$. The coefficient $p - p_s$ is intrinsic. The lifetime of the intermediate state lasts $T_s \propto -\omega_s^{-1}\ln|p - p_s|$. The final phase of the evolution is determined by the amplitude of the perturbation. If $p < p_s$, the system evolves into a BBH, but if $p > p_s$, the system eventually turns into a stable SBH. In both cases, we see in Fig.1, there are gaps in the scalar field on the horizon between unstable CS attractor and final stable configurations. The discontinuous change of the scalar field, when p passes through p_s , indicates the appearance of a first order phase transition in the critical scalarization. The dynamical critical phenomena disclosed here are similar to those in the EMS theory [17, 18].

Dynamical critical behaviors for descalarization. Now we start with a BBH, introduce a strong scalar perturbation to scalarize it and examine the nonlinear evolution of the SBH when p approaches p_d . The system heads to the CS at $p = p_d$. In Fig.2 we exhibit the dynamical evolution of the system. If $p < p_d$, the system smoothly and slowly evolves to a SBH. In Fig.3 we illustrate the scalar field evolution on the apparent horizon ϕ_h . When p approaches p_d from below, ϕ_h tends to a

constant and evolves extremely slow. It is still approximately described in a similar form to (7), but with the eigenvalue $\omega_d \simeq 0$, indicating that the CS near p_d is marginally stable. But if $p > p_d$, there is a jump in the scalar field value and the scalar hair is shedding off abruptly. The SBH is finally transformed into a BBH through a first-order phase transition.

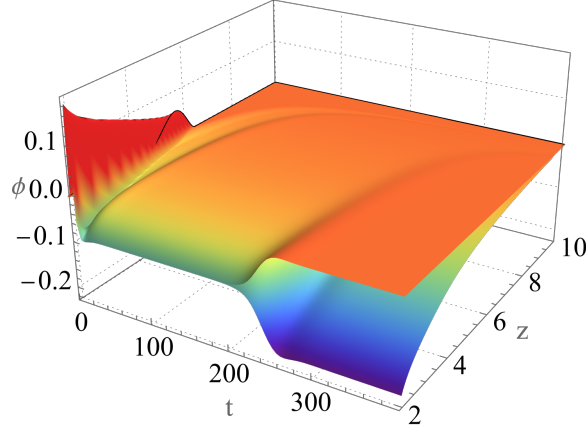


FIG. 1. The evolution of $\phi(t, r)$ near scalarization threshold p_s . Here $z = \frac{r}{1+r/L}$ is the compactified radial coordinate with $L = 10$. Initially, scalar pulse near the horizon violently interacts with the BBH. Then the system evolves to an attractor at $p = p_s$. Finally, the system forms a BBH if $p < p_s$ or a SBH if $p > p_s$. The upper and lower surfaces correspond to simulations with $p = p_s \mp e^{-28}$, respectively.

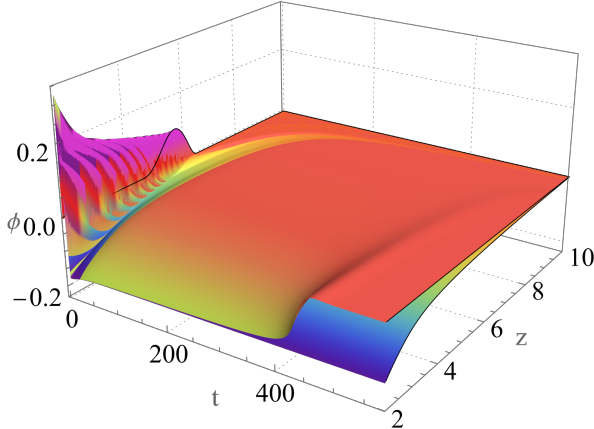


FIG. 2. The evolution of $\phi(t, r)$ near descalarization threshold p_d . The lower and upper surfaces correspond to the evolution starting with $p = 0.2438$ and $p = 0.2447$, respectively.

The critical behavior in the descalarization is different from that shown in Fig.1 for the scalarization. It does not agree to what observed in the EMS theory [17, 18] either. We find, for the first time, the marginally stable attractor in the descalarization. This critical dynamical behavior is also distinct from the usual type I critical gravitational collapse, which contains an unstable attractor at the threshold [19–22]. It is a new critical dynamical phenomenon disclosed in the

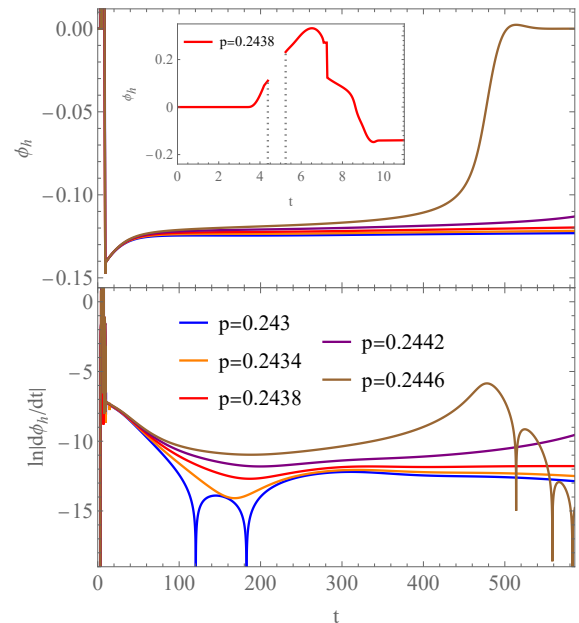


FIG. 3. The evolution of ϕ_h and $\ln |\frac{d\phi_h}{dt}|$ near threshold $p_d \approx 0.2438$. There is no unstable attractor during the evolution. The insets show that naked elliptic region appears when $t \in (4.38, 5.25)$ and there are no values of ϕ_h during this period for $p = 0.2438$.

first order phase transition.

In the generalized sGB theory, the null energy condition (NEC) is not always respected, which prevents the monotonic increasing of the Misner-Sharp (MS) mass and the BH horizon area with the radius and the time, respectively. Moreover, we perform hyperbolicity analysis in the fully nonlinear evolution and find that proper coupling between the scalar field and Ricci scalar can accommodate apparent horizon in time to hide the elliptic region and ensure the smooth numerical computation. The inset in the upper panel of Fig.3 shows the evolution of ϕ_h at early time, the time interval labelled by the dashed lines indicates the presence of naked elliptic region. For related discussion, please see supplemental material.

Numerical results for static solutions. To better understand the dynamical critical scalarization and descalarization, we work out the static solutions by solving the static equations of motion directly. For the numerical details please see supplemental material. The green curve in the top panel of Fig.4 indicates that the BBH is always a solution. Interestingly, when the mass is in appropriate range, there are extra two branches of SBH solutions. The red branch intersects with the BBH at $M = 0$ and with the blue branch at point (d) with mass $M_d \simeq 1.396$. From the perturbative analysis, we learn that the blue and green branches are linearly stable, while the red branch has unstable eigenmode with purely positive imaginary frequency, as shown in the bottom panel. Note that the static solution at (d) is marginally stable with zero mode $\omega_I = 0$. The middle panel shows the Wald entropy of the three branches, taking into account the scalar

field non-minimal coupling with Ricci scalar and GB term [52, 53]:

$$S = \pi r_h^2 [\beta f(\phi_h) + 1] + 4\pi f(\phi_h). \quad (8)$$

All the three branches have entropy increasing with M . The differences between them are tiny and are shown in the inset. The unstable SBH branch has always the smallest entropy. It intersects with the stable SBH branch at the cusp (d) of the swallow tail.

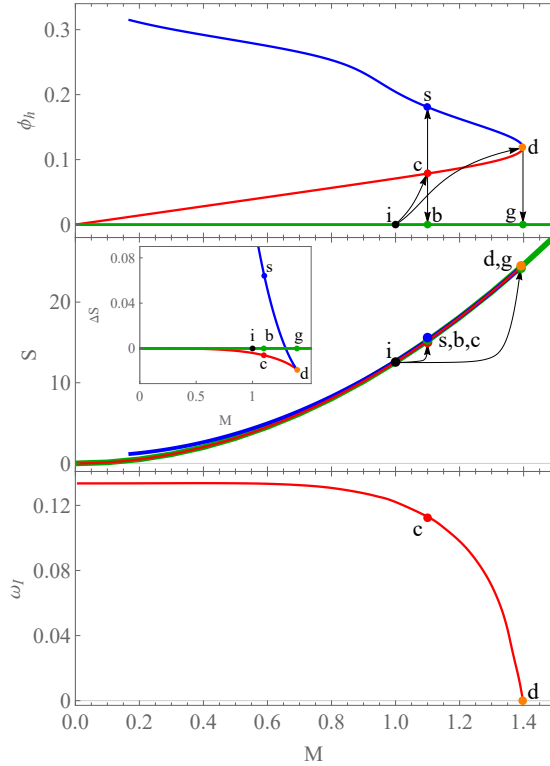


FIG. 4. The scalar value on the horizon ϕ_h , entropy S and the single unstable eigenmode frequency ω_I of the static solutions with respect to ADM mass M . The green, blue and red lines are results for stable BBH, SBH and unstable SBH solutions, respectively. There is no stable SBH when $M < 0.165$. The inset shows the entropy difference $\Delta S = S - S_B$ in which $S_B = 4\pi M^2$ is the entropy of the BBH. The upper and lower surfaces in Fig.1 correspond to schematic paths (i,c,b) and (i,c,s), respectively. The lower and upper surfaces in Fig.2 correspond to schematic paths (i,d) and (i,d,g), respectively.

Now we compare the dynamical results with the static solutions. The dynamical simulation starts from an initial BBH with $M_0 = 1$ under the perturbation (6) with the amplitude p . When p increases towards p_s from below, the final state stays on the green curve. The BBH becomes more massive in this process. When p approaches p_s , the scalar field starts to adhere onto the BBH and transform the BBH at (i) into an unstable SBH at (c). If $p < p_s$, the unstable SBH settles down to a heavier BBH described at point (b). However, if $p > p_s$ the unstable SBH evolves into a stable SBH at (s). The static solutions at points (c), (b) and (s) have the same mass $M_s = 1.098$. There are gaps between

scalar hair values in comparing unstable SBH at (c) with BBH at (b) or with stable SBH at (s). The unstable mode has eigenvalue $\omega_I \simeq 0.110$, in consist with the ω_s obtained in the evolution within the error tolerance. The appearance of the unstable SBH attractor repeats the property disclosed in the EMS theory [17]. When p approaches p_d from below, the SBH becomes marginally stable with zero mode at (d), agreeing with $\omega_d \simeq 0$ computed in the dynamical evolution. Once p passes across p_d , the final state jumps to the BBH at point (g), where the scalar hair is suddenly deprived. The BBH at (g) has the same mass as that of the marginally stable SBH at (d). At this transition point, the marginally stable CS acts as an attractor in the dynamical evolution.

Summary and discussion. In a general theory containing a scalar field interacting with the GB invariant, we demonstrated that the scalar-Ricci coupling improves the hyperbolic nature in the fully nonlinear dynamical evolution. We showed that such Ricci coupling has a positive effect in exploring hair formation and removal in dynamics. We disclosed the critical dynamics in the scalarization and descalarization in a theory possessing scalar-GB coupling. We showed that the scalarization of a Schwarzschild BH exhibits a typical type I dynamical critical behavior, in which an unstable attractor lives at the perturbation threshold, and a linearly stable BBH can be transformed through this CS and settle down in a final stable SBH. In the descalarization we uncovered a new critical phenomenon, where CS is a marginally stable SBH playing the role of an attractor in the evolution. This is a novel critical phenomenon in the first order phase transition. It is distinct from what observed in the EMS theory [17, 18]. From the perspective of thermodynamics, we found that the dynamical critical descalarization occurs at the cusp of swallow tail in the entropy-mass relation, where the static unstable SBH branch and the stable SBH branch meet, and a marginally stable SBH with zero mode lives. In the EMS theory, the dynamical descalarization occurs before the cusp [18]. To the best of our knowledge, this is the first example of marginal type I dynamical BH transition.

Considering that an abrupt first-order matter phase transition in some gravity systems can induce gravitational wave (GW) emission [54–57], it is of great interest to further investigate the critical dynamics in the first-order gravity phase transition in the generalized theory, whose mechanism could play an important role in the emission of GW.

Acknowledgments. This research is supported by National Key R&D Program of China under Grant No.2020YFC2201400, and the Natural Science Foundation of China under Grant Nos. 11975235, 12005077, 12035016 and Guangdong Basic and Applied Basic Research Foundation under Grant No. 2021A1515012374. B. W. was partially supported by NNSFC under grant 12075202. Some of our calculations were performed using the tensor-algebra bundle xAct [58].

^{*} yunqiliu@yzu.edu.cn (co-first author)
[†] zhangcy@email.jnu.edu.cn (co-first author)
[‡] chenqian192@mails.ucas.ac.cn
[§] zjcao@amt.ac.cn
[¶] ytian@ucas.ac.cn
^{**} wang_b@sjtu.edu.cn (corresponding author)

[1] D. D. Doneva and S. S. Yazadjiev, New Gauss-Bonnet Black Holes with Curvature-Induced Scalarization in Extended Scalar-Tensor Theories, *Phys. Rev. Lett.* **120**, no.13, 131103 (2018) [arXiv:1711.01187 [gr-qc]].

[2] H. O. Silva, J. Sakstein, L. Gualtieri, T. P. Sotiriou and E. Berti, Spontaneous scalarization of black holes and compact stars from a Gauss-Bonnet coupling, *Phys. Rev. Lett.* **120**, no.13, 131104 (2018) [arXiv:1711.02080 [gr-qc]].

[3] G. Antoniou, A. Bakopoulos and P. Kanti, Evasion of No-Hair Theorems and Novel Black-Hole Solutions in Gauss-Bonnet Theories, *Phys. Rev. Lett.* **120**, no.13, 131102 (2018) [arXiv:1711.03390 [hep-th]].

[4] P. V. P. Cunha, C. A. R. Herdeiro and E. Radu, “Spontaneously Scalarized Kerr Black Holes in Extended Scalar-Tensor–Gauss-Bonnet Gravity,” *Phys. Rev. Lett.* **123**, no.1, 011101 (2019) [arXiv:1904.09997 [gr-qc]].

[5] C. A. R. Herdeiro, E. Radu, H. O. Silva, T. P. Sotiriou and N. Yunes, “Spin-induced scalarized black holes,” *Phys. Rev. Lett.* **126**, no.1, 011103 (2021) [arXiv:2009.03904 [gr-qc]].

[6] E. Berti, L. G. Collodel, B. Kleihaus and J. Kunz, “Spin-induced black-hole scalarization in Einstein-scalar-Gauss-Bonnet theory,” *Phys. Rev. Lett.* **126**, no.1, 011104 (2021) [arXiv:2009.03905 [gr-qc]].

[7] A. Dima, E. Barausse, N. Franchini and T. P. Sotiriou, “Spin-induced black hole spontaneous scalarization,” *Phys. Rev. Lett.* **125**, no.23, 231101 (2020) [arXiv:2006.03095 [gr-qc]].

[8] C. A. R. Herdeiro, E. Radu, N. Sanchis-Gual and J. A. Font, “Spontaneous Scalarization of Charged Black Holes,” *Phys. Rev. Lett.* **121**, no.10, 101102 (2018) [arXiv:1806.05190 [gr-qc]].

[9] H. O. Silva, H. Witek, M. Elley and N. Yunes, “Dynamical Descalarization in Binary Black Hole Mergers,” *Phys. Rev. Lett.* **127**, no.3, 031101 (2021) [arXiv:2012.10436 [gr-qc]].

[10] M. Elley, H. O. Silva, H. Witek and N. Yunes, “Spin-induced dynamical scalarization, de-scalarization and stealthiness in scalar-Gauss-Bonnet gravity during black hole coalescence,” [arXiv:2205.06240 [gr-qc]].

[11] D. D. Doneva and S. S. Yazadjiev, “Beyond the spontaneous scalarization: New fully nonlinear mechanism for the formation of scalarized black holes and its dynamical development,” *Phys. Rev. D* **105**, no.4, L041502 (2022) [arXiv:2107.01738 [gr-qc]].

[12] J. L. Blázquez-Salcedo, D. D. Doneva, J. Kunz and S. S. Yazadjiev, “Radial perturbations of scalar-Gauss-Bonnet black holes beyond spontaneous scalarization,” [arXiv:2203.00709 [gr-qc]].

[13] D. D. Doneva, A. Vañó-Viñuales and S. S. Yazadjiev, “Dynamical descalarization with a jump during black hole merger,” [arXiv:2204.05333 [gr-qc]].

[14] J. L. Blázquez-Salcedo, C. A. R. Herdeiro, J. Kunz, A. M. Pombo and E. Radu, “Einstein-Maxwell-scalar black holes: the hot, the cold and the bald,” *Phys. Lett. B* **806**, 135493 (2020) [arXiv:2002.00963 [gr-qc]].

[15] J. Luis Blázquez-Salcedo, C. A. R. Herdeiro, S. Kahlen, J. Kunz, A. M. Pombo and E. Radu, “Quasinormal modes of hot, cold and bald Einstein–Maxwell-scalar black holes,” *Eur. Phys. J. C* **81**, no.2, 155 (2021) [arXiv:2008.11744 [gr-qc]].

[16] J. L. Blázquez-Salcedo, S. Kahlen and J. Kunz, “Critical solutions of scalarized black holes,” *Symmetry* **12**, no.12, 2057 (2020) [arXiv:2011.01326 [gr-qc]].

[17] C. Y. Zhang, Q. Chen, Y. Liu, W. K. Luo, Y. Tian and B. Wang, “Critical Phenomena in Dynamical Scalarization of Charged Black Holes,” *Phys. Rev. Lett.* **128**, no.16, 161105 (2022) [arXiv:2112.07455 [gr-qc]].

[18] C. Y. Zhang, Q. Chen, Y. Liu, W. K. Luo, Y. Tian and B. Wang, “Dynamical transitions in scalarization and descalarization through black hole accretion,” [arXiv:2204.09260 [gr-qc]].

[19] M. W. Choptuik, T. Chmaj and P. Bizon, “Critical behavior in gravitational collapse of a Yang-Mills field,” *Phys. Rev. Lett.* **77**, 424-427 (1996) [arXiv:gr-qc/9603051 [gr-qc]].

[20] S. L. Liebling and M. W. Choptuik, “Black hole criticality in the Brans-Dicke model,” *Phys. Rev. Lett.* **77**, 1424-1427 (1996) [arXiv:gr-qc/9606057 [gr-qc]].

[21] P. Bizon and T. Chmaj, “Critical collapse of Skyrmiions,” *Phys. Rev. D* **58**, 041501 (1998) [arXiv:gr-qc/9801012 [gr-qc]].

[22] C. Gundlach and J. M. Martin-Garcia, “Critical phenomena in gravitational collapse,” *Living Rev. Rel.* **10**, 5 (2007) [arXiv:0711.4620 [gr-qc]].

[23] B. Shiralilou, T. Hinderer, S. M. Nissanke, N. Ortiz and H. Witek, “Post-Newtonian gravitational and scalar waves in scalar-Gauss–Bonnet gravity,” *Class. Quant. Grav.* **39**, no.3, 035002 (2022) [arXiv:2105.13972 [gr-qc]].

[24] L. K. Wong, C. A. R. Herdeiro and E. Radu, “Constraining spontaneous black hole scalarization in scalar-tensor-Gauss-Bonnet theories with current gravitational-wave data,” *Phys. Rev. D* **106**, no.2, 024008 (2022) [arXiv:2204.09038 [gr-qc]].

[25] V. I. Danchev, D. D. Doneva and S. S. Yazadjiev, “Constraining scalarization in scalar-Gauss-Bonnet gravity through binary pulsars,” [arXiv:2112.03869 [gr-qc]].

[26] A. Maselli, N. Franchini, L. Gualtieri and T. P. Sotiriou, “Detecting scalar fields with Extreme Mass Ratio Inspirals,” *Phys. Rev. Lett.* **125**, no.14, 141101 (2020) [arXiv:2004.11895 [gr-qc]].

[27] H. Guo, Y. Liu, C. Zhang, Y. Gong, W. L. Qian and R. H. Yue, “Detection of scalar fields by extreme mass ratio inspirals with a Kerr black hole,” *Phys. Rev. D* **106**, no.2, 024047 (2022) [arXiv:2201.10748 [gr-qc]].

[28] S. Barsanti, N. Franchini, L. Gualtieri, A. Maselli and T. P. Sotiriou, “Extreme mass-ratio inspirals as probes of scalar fields: eccentric equatorial orbits around Kerr black holes,” [arXiv:2203.05003 [gr-qc]].

[29] J. L. Blázquez-Salcedo, D. D. Doneva, J. Kunz and S. S. Yazadjiev, “Radial perturbations of the scalarized Einstein-Gauss-Bonnet black holes,” *Phys. Rev. D* **98**, no.8, 084011 (2018) [arXiv:1805.05755 [gr-qc]].

[30] H. O. Silva, C. F. B. Macedo, T. P. Sotiriou, L. Gualtieri, J. Sakstein and E. Berti, “Stability of scalarized black hole solutions in scalar-Gauss-Bonnet gravity,” *Phys. Rev. D* **99**, no.6, 064011 (2019) [arXiv:1812.05590 [gr-qc]].

[31] S. Hod, “Onset of spontaneous scalarization in spinning Gauss-Bonnet black holes,” *Phys. Rev. D* **102**, no.8, 084060 (2020) [arXiv:2006.09399 [gr-qc]].

[32] J. L. Ripley and F. Pretorius, “Hyperbolicity in Spherical Gravitational Collapse in a Horndeski Theory,” *Phys. Rev. D* **99**, no.8, 084014 (2019) [arXiv:1902.01468 [gr-qc]].

[33] J. L. Ripley and F. Pretorius, “Gravitational collapse in Einstein dilaton-Gauss–Bonnet gravity,” *Class. Quant. Grav.* **36**, no.13, 134001 (2019) [arXiv:1903.07543 [gr-qc]].

[34] F. L. Julié and E. Berti, “ $d+1$ formalism in Einstein-scalar-Gauss-Bonnet gravity,” *Phys. Rev. D* **101**, no.12, 124045 (2020)

[arXiv:2004.00003 [gr-qc]].

[35] H. Witek, L. Gualtieri and P. Pani, “Towards numerical relativity in scalar Gauss-Bonnet gravity: $3+1$ decomposition beyond the small-coupling limit,” Phys. Rev. D **101**, no.12, 124055 (2020) [arXiv:2004.00009 [gr-qc]].

[36] W. E. East and J. L. Ripley, “Evolution of Einstein-scalar-Gauss-Bonnet gravity using a modified harmonic formulation,” Phys. Rev. D **103**, no.4, 044040 (2021) [arXiv:2011.03547 [gr-qc]].

[37] H. Witek, L. Gualtieri, P. Pani and T. P. Sotiriou, “Black holes and binary mergers in scalar Gauss-Bonnet gravity: scalar field dynamics,” Phys. Rev. D **99**, no.6, 064035 (2019) [arXiv:1810.05177 [gr-qc]].

[38] D. D. Doneva and S. S. Yazadjiev, “Dynamics of the nonrotating and rotating black hole scalarization,” Phys. Rev. D **103**, no.6, 064024 (2021) [arXiv:2101.03514 [gr-qc]].

[39] J. L. Ripley and F. Pretorius, “Dynamics of a \mathbb{Z}_2 symmetric EdGB gravity in spherical symmetry,” Class. Quant. Grav. **37**, no.15, 155003 (2020) [arXiv:2005.05417 [gr-qc]].

[40] H. J. Kuan, D. D. Doneva and S. S. Yazadjiev, “Dynamical Formation of Scalarized Black Holes and Neutron Stars through Stellar Core Collapse,” Phys. Rev. Lett. **127**, no.16, 161103 (2021) [arXiv:2103.11999 [gr-qc]].

[41] W. E. East and J. L. Ripley, “Dynamics of Spontaneous Black Hole Scalarization and Mergers in Einstein-Scalar-Gauss-Bonnet Gravity,” Phys. Rev. Lett. **127**, no.10, 101102 (2021) [arXiv:2105.08571 [gr-qc]].

[42] Y. Liu, C. Y. Zhang, W. L. Qian, K. Lin and B. Wang, “Dynamic generation or removal of a scalar hair,” [arXiv:2206.05012 [gr-qc]].

[43] N. Franchini, M. Bezares, E. Barausse and L. Lehner, “Fixing the dynamical evolution in scalar-Gauss-Bonnet gravity,” [arXiv:2206.00014 [gr-qc]].

[44] G. Antoniou, C. F. B. Macedo, R. McManus and T. P. Sotiriou, “Stable spontaneously-scalarized black holes in generalized scalar-tensor theories,” [arXiv:2204.01684 [gr-qc]].

[45] T. Damour and G. Esposito-Farese, Nonperturbative strong field effects in tensor-scalar theories of gravitation, Phys. Rev. Lett., vol. 70, pp. 2220-2223.

[46] T. Damour and G. Esposito-Farese, “Tensor-scalar gravity and binary pulsar experiments,” Phys. Rev. D **54** (1996), 1474-1491 [arXiv:gr-qc/9602056 [gr-qc]].

[47] T. Harada, “Stability analysis of spherically symmetric star in scalar-tensor theories of gravity,” Prog. Theor. Phys. **98** (1997), 359-379 [arXiv:gr-qc/9706014 [gr-qc]].

[48] G. Antoniou, L. Bordin and T. P. Sotiriou, “Compact object scalarization with general relativity as a cosmic attractor,” Phys. Rev. D **103**, no.2, 024012 (2021) [arXiv:2004.14985 [gr-qc]].

[49] G. Ventagli, G. Antoniou, A. Lehébel and T. P. Sotiriou, “Neutron star scalarization with Gauss-Bonnet and Ricci scalar couplings,” Phys. Rev. D **104**, no.12, 124078 (2021) [arXiv:2111.03644 [gr-qc]].

[50] G. Antoniou, A. Lehébel, G. Ventagli and T. P. Sotiriou, “Black hole scalarization with Gauss-Bonnet and Ricci scalar couplings,” Phys. Rev. D **104**, no.4, 044002 (2021) [arXiv:2105.04479 [gr-qc]].

[51] G. Ventagli, A. Lehébel and T. P. Sotiriou, “Onset of spontaneous scalarization in generalized scalar-tensor theories,” Phys. Rev. D **102**, no.2, 024050 (2020) [arXiv:2006.01153 [gr-qc]].

[52] R. M. Wald, “Black hole entropy is the Noether charge,” Phys. Rev. D **48**, no.8, R3427-R3431 (1993) [arXiv:gr-qc/9307038 [gr-qc]].

[53] V. Iyer and R. M. Wald, “Some properties of Noether charge and a proposal for dynamical black hole entropy,” Phys. Rev. D **50**, 846-864 (1994) [arXiv:gr-qc/9403028 [gr-qc]].

[54] E. R. Most, L. J. Papenfort, V. Dexheimer, M. Hanuske, S. Schramm, H. Stöcker and L. Rezzolla, Phys. Rev. Lett. **122**, no.6, 061101 (2019) doi:10.1103/PhysRevLett.122.061101 [arXiv:1807.03684 [astro-ph.HE]].

[55] A. Bauswein, N. U. F. Bastian, D. B. Blaschke, K. Chatzioannou, J. A. Clark, T. Fischer and M. Oertel, Phys. Rev. Lett. **122**, no.6, 061102 (2019) doi:10.1103/PhysRevLett.122.061102 [arXiv:1809.01116 [astro-ph.HE]].

[56] L. R. Weih, M. Hanuske and L. Rezzolla, Phys. Rev. Lett. **124**, no.17, 171103 (2020) doi:10.1103/PhysRevLett.124.171103 [arXiv:1912.09340 [gr-qc]].

[57] S. Zha, E. P. O’Connor, M. c. Chu, L. M. Lin and S. M. Couch, Phys. Rev. Lett. **125**, no.5, 051102 (2020) [erratum: Phys. Rev. Lett. **127**, no.21, 219901 (2021)] doi:10.1103/PhysRevLett.127.219901 [arXiv:2007.04716 [astro-ph.HE]].

[58] xAct: Efficient tensor computer algebra for the Wolfram Language, <http://www.xact.es/>.

[59] C. Y. Zhang, P. Liu, Y. Liu, C. Niu and B. Wang, “Evolution of anti-de Sitter black holes in Einstein-Maxwell-dilaton theory,” Phys. Rev. D **105**, no.2, 024010 (2022) [arXiv:2104.07281 [gr-qc]].

[60] C. Y. Zhang, P. Liu, Y. Liu, C. Niu and B. Wang, “Dynamical scalarization in Einstein-Maxwell-dilaton theory,” Phys. Rev. D **105**, no.2, 024073 (2022) [arXiv:2111.10744 [gr-qc]].

[61] C. W. Misner and D. H. Sharp, “Relativistic equations for adiabatic, spherically symmetric gravitational collapse,” Phys. Rev. **136**, B571-B576 (1964)

[62] S. W. Hawking and G. F. R. Ellis. The Large Scale Structure of Space-Time (Cambridge Monographs on Mathematical Physics). Cambridge University Press, 1975.

[63] J. M. Bardeen, B. Carter, and S. W. Hawking. The four laws of black hole mechanics. Communications in Mathematical Physics, 31:161-170, June 1973.

[64] S. A. Hayward. General laws of black-hole dynamics. Phys. Rev. D, 49:6467-6474, Jun 1994.

[65] A. Ashtekar and B. Krishnan, “Isolated and dynamical horizons and their applications,” Living Rev. Rel. **7**, 10 (2004) [arXiv:gr-qc/0407042 [gr-qc]].

SUPPLEMENTAL MATERIAL

Details for numerical simulation. We first show the details for the full nonlinear dynamical simulation. Defining auxiliary variables

$$Q = \partial_r \phi, \quad P = \frac{1}{\alpha} \partial_t \phi - \zeta Q. \quad (9)$$

we get evolution equations

$$E_\phi \equiv \partial_t \phi - \alpha (P + Q\zeta) = 0, \quad (10)$$

$$E_Q \equiv \partial_t Q - \partial_r [\alpha(P + Q\zeta)] = 0, \quad (11)$$

$$E_P \equiv \partial_t P - A_P = 0, \quad (12)$$

$$E_\zeta \equiv \partial_t \zeta - A_\zeta = 0, \quad (13)$$

and constraint equations

$$\alpha' = C_\alpha, \quad \zeta' = C_\zeta. \quad (14)$$

Here $A_{P,\zeta}, C_{\alpha,\zeta}$ are lengthy expressions of $\phi, P, Q, \alpha, \zeta$ and their radial derivatives. Given initial data ϕ_0, P_0 , we can work out initial Q from (9) and α, ζ from (14). Then by using (10, 11, 12), we can work out the ϕ, Q, P on the next time slice. Iterating this procedure, we get all variables on all time slices. The equation (13) is auxiliary. The constraints (14) are solved with the Newton-Raphson method. The evolution equations (10, 11, 12) are solved with method of lines, in which the radial derivative is discretized with fourth-order finite difference method and the time direction is evolved with fourth-order Runge-Kutta method. The Courant-Friedrichs-Lowy condition is satisfied. The Kress-Oliger dissipation is employed to stabilize the code.

With the gauge freedom $\alpha \rightarrow l\alpha, t \rightarrow t/l$ in the metric, we can set $\alpha|_{r \rightarrow \infty} = 1$. This implies that we take the time coordinate t as the proper time of the observer at spatial infinity. The metric function $\zeta \rightarrow \sqrt{\frac{2M}{r}}$ at large radius. Here M is the total mass of the spacetime. To improve the stability of our numerical code, we use variable $s = \sqrt{r}\zeta$ and impose the boundary condition $s|_{r \rightarrow \infty} = \sqrt{2M}$ in the code.

We compactify the radial direction as $z = \frac{r}{1+r/L}$ in which $L = 10M_0$, and discretize z with a uniform grid. On each time slice, the computational domain covers $z \in [z_e, L]$ where z_e denotes the inner boundary and locates at a few distance inside the apparent horizon.

The convergence order q of our method can be estimated by $\frac{V_{2N} - V_N}{V_{4N} - V_{2N}} = 2^q + O(1/N)$. Here V_N is the result obtained with N radial grid points. As shown in Fig.5, our method converges to the second order. The dynamical simulations shown in the main text are obtained with $N = 4096$.

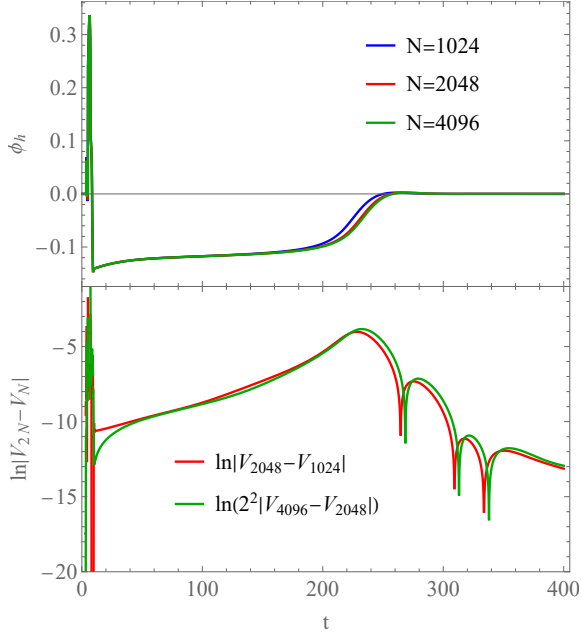


FIG. 5. The evolution of ϕ_h with different grid points N when $p = 0.246$. The differences $V_{2048} - V_{1024}$ almost overlaps with the four times of $V_{4096} - V_{2048}$.

Hyperbolicity. Now let us consider the hyperbolicity of the scalar field equation. The radial characteristic speeds $c_{\pm} = \mp\xi_t/\xi_r$ of the scalar field ϕ are determined by characteristic equation

$$\det \left[\begin{pmatrix} \frac{\delta E_P}{\delta(\partial_a P)} & \frac{\delta E_P}{\delta(\partial_a Q)} \\ \frac{\delta E_Q}{\delta(\partial_a P)} & \frac{\delta E_Q}{\delta(\partial_a Q)} \end{pmatrix} \xi_a \right] = 0, \quad (15)$$

in which $\xi_a = (\xi_t, \xi_r)$. This equation has quadratic form $\mathcal{A}c^2 + \mathcal{B}c + \mathcal{C} = 0$ in which $\mathcal{A}, \mathcal{B}, \mathcal{C}$ are complicated functions of the metric and scalar field [32, 33, 39]. The regions of spacetime where the discriminant $\mathcal{D} \equiv \mathcal{B}^2 - 4\mathcal{A}\mathcal{C} < 0$ are elliptic regions. If elliptic region appears, we excise it and shift the inner boundary z_e at the next time slice. Sometimes naked elliptic region appears outside the apparent horizon. This was also encountered in sGB theory with other coupling functions [32, 33, 39]. In general, the naked elliptic region disables the time evolution. However, if the apparent horizon increases in time and hides the elliptic region, it will prevent the pathological region from affecting the outside world, so that we can continue the simulation, as shown in Fig.6. Similar situation was encountered in the Einstein-Maxwell-dilaton theory for simulation starting from an initial spacetime with naked singularity [59, 60]. Nevertheless, if the apparent horizon is unable to hide the elliptic region in time, the code will crash. This happens for simulations with $\beta > -1.5$. Fig.6 provides evidence that in the fully dynamical process

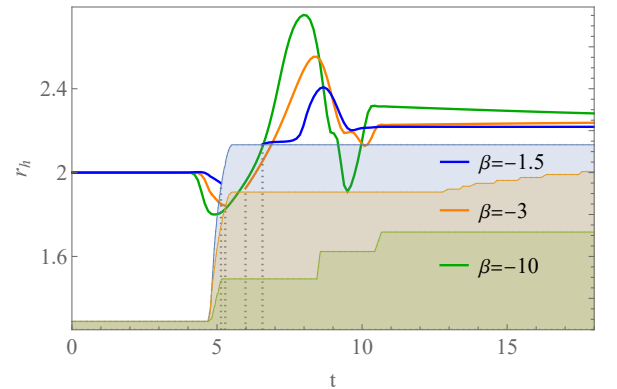


FIG. 6. The evolution of the apparent horizon r_h and excision region for various β when $M_0 = 1, p = 0.14$. The light blue, orange and green regions are results for $\beta = -1.5, -3, -10$, respectively.

the coupling with R can indeed reduce the elliptic or excision region. This result generalizes the result in the linear analysis [44]. When $\beta = 0$, the theory returns to the sGB theory where the scalarizations were reported in [11–13]. Reference [44] limits the discussion in the linear level, where the fully nonlinear dynamical critical behaviors were not examined.

Violation of null energy condition. Now we examine the quasi-local Misner-Sharp (MS) mass $M_{MS}(t, r) \equiv \frac{r}{2}(1 - \nabla_a r \nabla^a r) = \frac{1}{2}r\zeta^2$ [61]. It equals the radial integral of the effective energy density [33]. For the model we consider, the effective stress tensor (3) does not always satisfy the usual

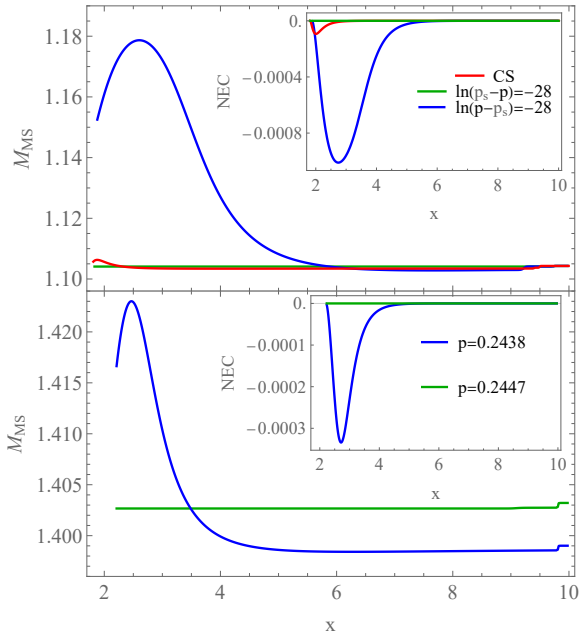


FIG. 7. The distribution of the MS mass for SBHs (blue), Schwarzschild BHs (green) and CS (red). The insets indicate the violation of the NEC for SBHs and CS.

energy conditions such as the null energy condition (NEC) $T_{\mu\nu}l^\mu l^\nu \geq 0$ for an outgoing null vectors $l^\mu = (1, -\alpha, 0, 0)$. This implies that the MS mass and the BH horizon area do not always monotonically increase with radius [33, 39] and time [62–65], respectively. The MS mass distributions in the CS, the final SBH and BBH are shown in Fig.7. The MS mass increases near the horizon and then decreases with radius, implying that there is a negative effective energy density distribution in the space [33, 39]. Note that this follows not from the presence of an exotic form of matter but from the synergy of the scalar field coupling with the GB term.

In the main text, we focused on the evolution of the scalar value on the apparent horizon. Now we consider the evolution of the apparent horizon area radius. Fig.8 shows that the BH apparent horizon area can decrease during the evolution. Especially, the upper panel indicates that the CS has a larger horizon area than the final BBH. This is not surprising because the violation of NEC leads to the breakdown of the BH area theorem [62–65]. Nevertheless, the synergy of a scalar field coupling with both the Ricci scalar and GB invariant affects the final solutions which presents larger Wald entropy than that of the CS and the initial BH, as shown in Fig.4. Besides, we find that the relation $\ln \dot{r}_h \propto 2 \ln |\dot{\phi}_h|$ found in the EMS theory [17, 18] does not hold here.

Details for solving static solutions and perturbations. At last, we present the numerical procedure for solving the static solutions and quasinormal frequencies. For convenience we

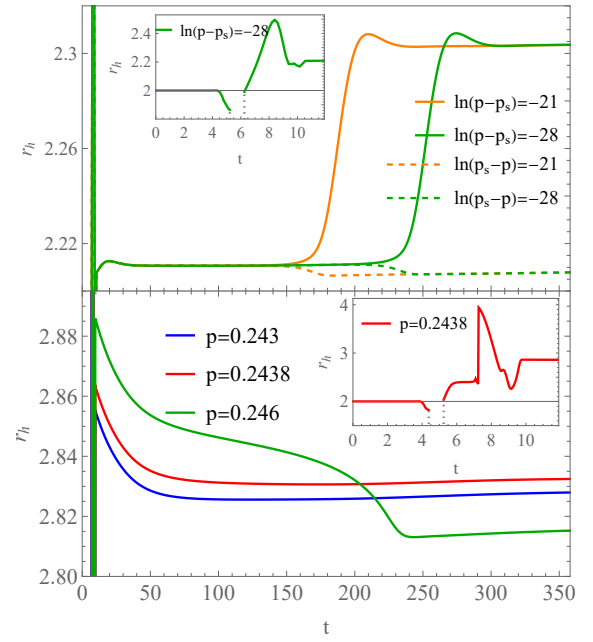


FIG. 8. The evolution of apparent horizon r_h near thresholds p_s and p_d . The upper and lower insets show that naked elliptic regions appear when $t \in (5.23, 6.25)$ and $t \in (4.38, 5.25)$ and there are no values of r_h during these periods for $\ln(p - p_s) = -28$ and $p = 0.2438$, respectively.

use the following metric ansatz [29, 30].

$$ds^2 = -e^{\Lambda(r) + \epsilon F_t(t_s, r)} dt_s^2 + e^{T(r) + \epsilon F_r(t_s, r)} dr^2 + r^2 (dr^2 + \sin^2 \theta d\varphi^2), \quad (16)$$

$$\phi(t_s, r) = \phi_0(r) + \epsilon \phi_1(t_s, r). \quad (17)$$

Here ϵ is an infinitesimal perturbation parameter. The zeroth order terms in the equations of motion govern static background functions Λ , T and ϕ_0 , while the first order terms govern time-dependent perturbation functions F_t , F_r and ϕ_1 . At static case, the coordinate transformation between (5) and (16) takes $dt_s = dt - \frac{\zeta dr}{(1 - \zeta^2)^\alpha}$. Note that the ϕ_h , S and ω_I do not change under this transformation.

From the zeroth order terms, the field equations of Λ , T and ϕ_0 are cast into three coupled ordinary differential equations (ODEs). After some algebra calculations, we obtain two coupled second-order ODEs for Λ and ϕ_0 , and an algebraic equation for T . We compact the radial coordinate as $x = 1 - \frac{r_h}{r}$. The boundary conditions are imposed as $e^\Lambda|_{x \rightarrow 0} \rightarrow 0$ and $e^{-T}|_{x \rightarrow 0} \rightarrow 0$ on the BH horizon, and $\phi_0|_{x \rightarrow 1} \rightarrow 0$ at infinity. After solving the equations, one can rescale $e^\Lambda|_{x \rightarrow 1} \rightarrow 1$ at infinity by the gauge freedom. The asymptotic behavior of the scalar field takes $\phi \sim \frac{D}{r} + O(r^{-2})$, where D denotes the scalar charge. Specifying D , λ , κ , β and r_h , we can obtain Λ and ϕ_0 by shooting method. The metric function T is then obtained as a function of Λ and ϕ_0 .

From the first order terms, after algebraic calculation, the scalar perturbation ϕ_1 decouples from the metric perturbations F_t and F_r [29, 30]. It has a single second order differential

equation which can be used to compute the quasinormal modes of the background solutions. With the decomposition $\phi_1(t_s, r) = \psi_1(r)e^{i\omega t_s}$, the scalar perturbation equation reads

$$[\partial_r^2 + A(r)\partial_r + (\omega^2 B(r)^2 - U(r))]\psi_1(r) = 0. \quad (18)$$

Here the coefficients $A(r)$, $B(r)$ and $U(r)$ are complicated functions depending on the background metric and scalar field Λ , T and ϕ_0 . We will focus on perturbations with purely imaginary eigenfrequencies that $\omega = i\omega_I$. ω_I can be obtained with the same method described in [29, 30].